Annals of Biomedical Engineering, Vol. 37, No. 9, September 2009 *(© 2009)* pp. 1839–1848
DOI: 10.1007/s10439-009-9735-9

On the Efficacy of the Combined Use of the Cross-Bicoherence with Surrogate Data Technique to Statistically Quantify the Presence of Nonlinear Interactions

KIN L. SIU and KI H. CHON

Department of Biomedical Engineering, SUNY at Stony Brook, HSC T18, Rm. 030, Stony Brook, NY, USA

(Received 18 February 2009; accepted 2 June 2009; published online 12 June 2009)

Abstract—The cross-bispectrum is an approach to detect the presence of quadratic phase coupling (QPC) between different components in bivariate signals. Quantification of QPC is by means of the cross-bicoherence index (CBI). The major limitations of the CBI are that it favors only the strongly coupled signals and its accuracy becomes compromised with noise and low coupling strength. To overcome this limitation, a statistical approach which combines CBI with a surrogate data method to determine the statistical significance of the QPC derived from bivariate signals is introduced. We demonstrate the accuracy of the proposed approach using simulation examples which are designed to test its robustness against noise contamination as well as varying levels of phase coupling and data lengths. Comparisons were made to the traditional CBI and the method based on the use of cross-bispectrum followed by a surrogate data technique. Our results show that the cross-bicoherence with surrogate data technique outperforms the two other methods compared in both sensitivity and specificity, and provides an unbiased and statistical approach to determining the presence of QPC in bivariate signals. These results are in contrast to our recent study where the auto-bispectrum combined with surrogate data approach had the best performance. Application of this approach to renal hemodynamic data was applied to renal stop flow pressure data obtained in the nephrons of the normotensive ($N = 18$) and hypertensive ($N = 15$) rats. We found significant nonlinear interactions between nephrons only when they are derived from the same cortical renal artery. The accuracy was 100% and verified by comparing the results to the known vascular connectivity between nephrons.

Keywords—Cross-bispectrum, Quadratic phase coupling, Cross-bicoherence, Nonlinear interactions, Surrogate data, Myogenic, TGF.

Address correspondence to Ki H. Chon, Department of Biomedical Engineering, SUNY at Stony Brook, HSC T18, Rm. 030, Stony Brook, NY 11794-8181, USA. Electronic mail: ki.chon@sunysb.edu

INTRODUCTION

In our previous work, nonlinear coupling between tubuloglomerular feedback (TGF) and the myogenic (MYO) mechanisms within a single nephron[11,15] as well as the whole kidney level[2,11] was detected for both normotensive and spontaneously hypertensive rats (SHRs) using a bispectrum approach. The reason for the interest in the detection of nonlinear interactions is that they can give rise to a number of system properties, including chaos, synchronization, and frequency modulation,[16] which may be physiologically important, and which do not occur in linear systems. The bispectrum is an algorithm used to detect both frequency and phase coupling between different components of a signal and bispectral peaks should only appear when these two criteria have been met.[9] However, in practice, having only the frequency coupling or insufficient segment averaging can lead to erroneous bispectral peaks. A long held dogma is that these erroneous peaks can be rejected by the use of a bicoherence index, but its determination of significant peaks favors only those with strong coupling. To overcome this limitation, we recently developed an algorithm which combines the bispectrum with surrogate data method to determine the statistical significance of the phase coupling.[15] Our approach completely bypasses the use of the bicoherence index. Our method showed far greater sensitivity and specificity than the bicoherence index and paved a way for an unbiased and statistical approach to determine the presence of quadratic phase coupling (QPC).

For bivariate signals, the cross-bispectrum can be used to detect QPC between dynamic components from two different signals. For example, it will be possible to detect coupling between the autoregulatory mechanisms from different nephrons.[15] Our aim is to apply the cross-bispectrum to examine if there are any differences in nephron-to-nephron interactions between normotensive and hypertensive rats.

Inherent weaknesses of the cross-bispectrum are nearly identical to those of the auto-bispectrum. For example, the cross-bispectrum also requires a sufficient number of segments to detect proper phase coupling. If these are not available, non-phase coupled components will appear in the resulting cross-bispectra, confounding the interpretation of the results. The most widely used approach to suppress these non-phase coupled peaks is via the cross-bicoherence index (CBI). Using multiple realizations of Gaussian white noise (GWN) signals, Shils *et al.*[14] provided a quantitative approach to determine a 95% significance level to discriminate between erroneous and true phase coupled peaks, based on the number of segments used. However, the main disadvantage of this approach is that the distribution of white noise is different than the data. In addition, the significance level derived by the white noise is a stringent criterion and may miss weak couplings between two signals, thereby leading to type II error.

Given the aforesaid limitations and the fact that we found a solution to selection of the significance of the determined auto-bispectral peaks based on a surrogate data technique, we initially assumed the same method can be used for cross-bispectrum. That is, first calculate the cross-bispectrum followed by surrogate data to determine the statistical significance of the calculated cross-bispectral peaks. Note that in our recent study, it was found that using the auto-bispectrum followed by surrogate data to determine the statistical significance was more accurate than using either the conventional bicoherence index or bicoherence followed by the surrogate data.[15] Similar to the auto-bispectrum case, we expected poor performance of the CBI for quantitative determination of the significance of the cross-bispectrum. To our surprise, the most accurate approach for auto-bispectrum (bispectrum followed by surrogate data) was not as effective for cross-bispectrum. Thus, the aim of the present study was to systematically investigate and compare three different approaches to determine the most accurate way to assess the significance of the estimated cross-bispectral peaks. The three methods compared are: (1) cross-bicoherence index (CBI), (2) cross-bispectrum with surrogate (CBS) data, and (3) cross-bicoherence with surrogate data. We have previously shown that the method of using bicoherence followed by the surrogate data works better than using only the bicoherence, but its accuracy was lower than the bispectrum with surrogate data approach.[15] Note that the second and third methods as defined above differ in that the former method uses cross-bispectral values whereas the latter method uses the cross-bicoherence values to determine the statistical significance.

To quantitatively compare three methods, computer simulations involving their effectiveness against varying levels of noise, coupling, and data lengths were investigated. Unlike the auto-bispectrum, it was found that the approach of cross-bicoherence with surrogate data performed the best for all test conditions considered. The technique of the cross-bicoherence with surrogate data was applied to stop flow pressure measurements obtained from two nephrons simultaneously in both normotensive and hypertensive rats to detect and discern quantitative differences in the QPC between two conditions.

METHODS

Cross-Bispectral Analysis

Given two stationary zero mean processes, $x(n)$ and $y(n)$, the direct method of computing the cross-bispectrum, B_{xyx}, involves taking the average of triple products of the Fourier transform over M segments:

$$B_{xyx}(\omega_1,\omega_2)=\frac{1}{M}\sum_{m=1}^{M}X^m(\omega_1)Y^m(\omega_2)X^{m*}(\omega_1+\omega_2) \tag{1}$$

where $X^m(\omega_1)$ and $Y^m(\omega_2)$ are the Fourier transform of the m-th segment and * indicates the complex conjugate.

Similar to auto-bispectrum, the cross-bispectrum will reveal peaks when QPC occurs between the two signals. An example of the QPC via the cross-bispectrum is illustrated in Fig. 1 using the following example[10]:

$$\begin{aligned} x_1(n) &= e^{j(2\pi f_x(1)n\Delta+\phi_x(1))}\\ x_2(n) &= e^{j(2\pi f_x(2)n\Delta+\phi_x(2))}\\ y_1(n) &= e^{j\left(2\pi f_y(1)n\Delta+\phi_y(1)\right)}\\ y_2(n) &= e^{j\left(2\pi f_y(2)n\Delta+\phi_y(2)\right)}\\ x(n) &= x_1(n)+x_2(n)+x_1(n)x_2(n)\\ y(n) &= y_1(n)+y_2(n)+y_1(n)x_2(n) \end{aligned} \tag{2}$$

The signals $x(n)$ and $y(n)$ are the two composite outputs of the simulation. In this simulation, the frequencies are set to: $f_x(1)=f_y(1)=0.03$ Hz and $f_x(2)=f_y(2)=0.12$ Hz to simulate the slow and fast mechanisms of renal autoregulation. Thirty-two segments of 128 data points of both $x(n)$ and $y(n)$ were generated (for a total of $n=4096$ data points and step size $\Delta=1$ s each), with the initial phase of each segment, ϕ, randomly distributed along 0 and 2π. Phase coupling is unidirectional from $y(n)$ to $x(n)$, with the third term in $y(n)$ being responsible for the

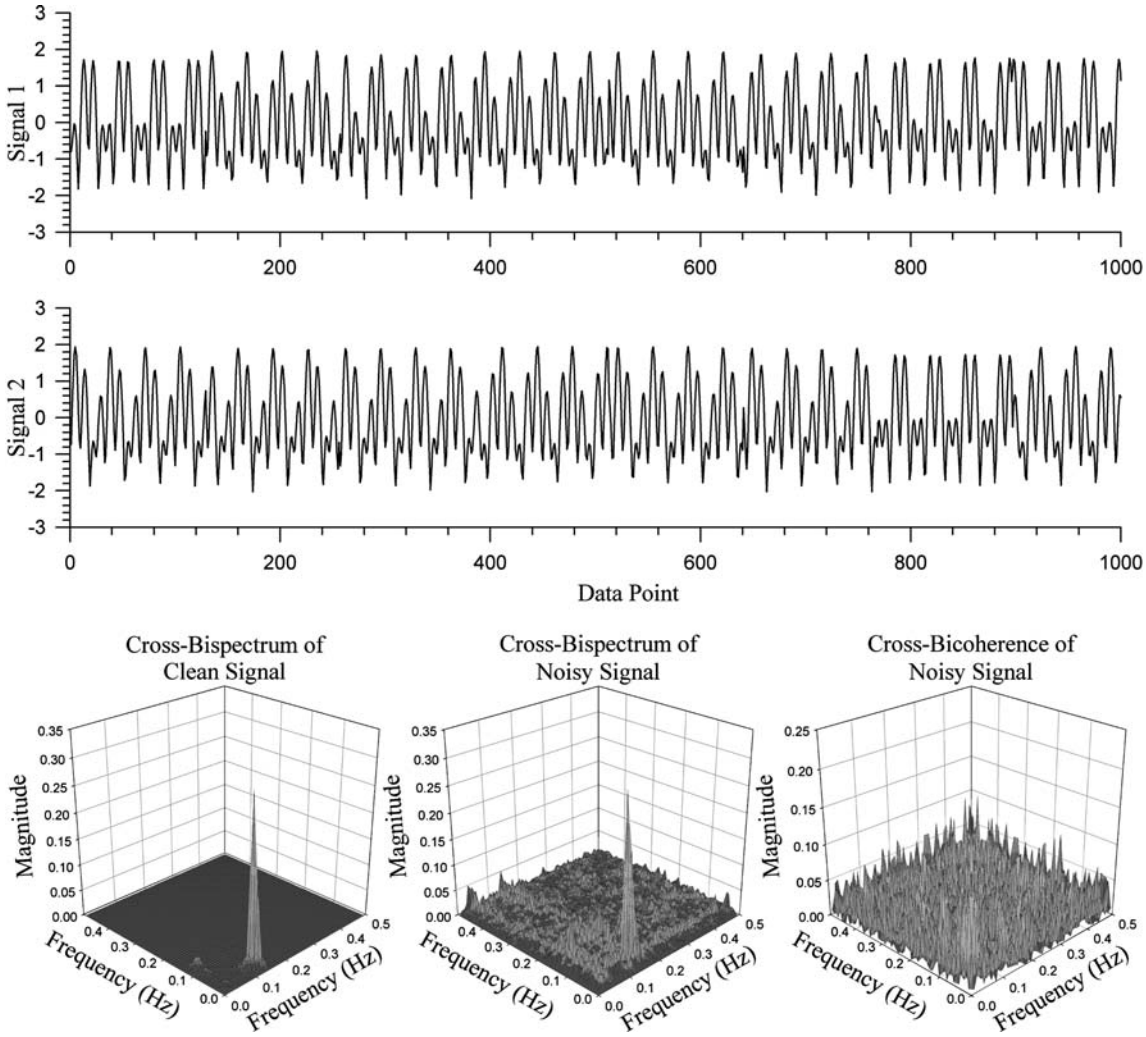

FIGURE 1. Simulation demonstrating the necessity of a new quantification method for the cross-bispectrum. The top two panels show a pair of simulated signals that are phase coupled with each other. The bottom left and middle panels show the cross-bispectrum of a pair of clean and noisy signals, respectively. Noise confounds interpretation of the results as shown in the bottom right panel even with the use of cross-bicoherence index.

coupling. Note that the simulated signals have imaginary portions. For visualization purposes, only the real portion of the signals is shown in the top two panels of Fig. 1. The bottom left panel shows the resulting cross-bispectra for these two simulated signals. Note that a single large peak is shown at the (0.03, 0.12) Hz frequency pair, suggesting significant phase coupling between the signals. The example provided was free of noise. More realistic example is to contaminate the signals as described in Eq. (2) with GWN. The signal-to-noise (SNR) ratio was set to −20 dB. The result is shown in the middle panel of Fig. 1. While the largest peak is the coupled peak, with such a low SNR, we observe many noise-related peaks in the cross-bispectrum.

To address how one can comb through to find only the significant phase coupled peak, the most widely used approach is a CBI, which is essentially a normalized cross-bispectrum:

$$bic_{xyx}(\omega_1, \omega_2) = \frac{B_{xyx}(\omega_1, \omega_2)}{\sqrt{P_x(\omega_1)P_y(\omega_2)P_x(\omega_1 + \omega_2)}} \quad (3)$$

where bic_{xyx} denotes the cross-bicoherence and P denotes the power spectrum. Shils *et al.*[14] introduced a 95% threshold of $\sqrt{3}/\sqrt{N}$, where N is the number of segments. Using this threshold value for the simulation above, we would erroneously reject the true phase coupled peak at (0.03, 0.12) Hz frequency pair, as illustrated in the right panel of Fig. 1. This type II error is likely due to the fact that the above-defined 95% threshold value is too stringent since it was based on GWN simulations, thus it is not able to discern a phase coupling that is contaminated by significant noise. While not shown, a similar type II error would

occur when the magnitude of the phase coupled peak is weak. These issues will be further illustrated in the "Results" section.

To circumvent this white noise based 95% threshold value of the CBI, we demonstrate utility of two methods that utilize the concept of surrogate data technique. Specifically, the two methods utilize a surrogate data testing approach to determine the statistical significant threshold value for either the cross-bispectrum or cross-bicoherence values. Surrogate data technique generates multiple random realizations of signal from real data that contain only the linear characteristics from the original signal. In essence, the surrogate data will not contain the phase couplings that are in the original signals, and can therefore be used as the null condition for statistical comparison. We chose the iteratively refined surrogate data technique (IRSDT).[19] The IRSDT will destroy any nonlinearity in the signal, and has been shown to be more accurate than the amplitude adjusted Fourier transform technique[18] because it iteratively corrects for deviations in the spectrum present in the amplitude adjusted Fourier transform technique as well as maintains the correct distribution of the signal.[13]

One hundred realizations of surrogate data pairs were generated, and the cross-bispectrum and cross-bicoherence values were calculated for each of the two methods. The mean and standard deviation between the 100 cross-bispectra or cross-bicoherence indices were then calculated, and the threshold was set to be the mean plus 2 standard deviations of the maximum peak in the cross-bispectrum or cross-bicoherence values. The magnitude of coupling is determined to be the difference between the original bispectrum and the calculated threshold. Using this method, the threshold for the cross-bispectrum is statistically determined and not based on arbitrary decision. The surrogate method based on the cross-bispectrum will henceforth be termed cross-bispectrum with surrogate (CBS) and the surrogate method based on the cross-bicoherence will henceforth be called CBicS.

Simulation Procedures

Computer generated data were used to compare the efficacy of the three methods. In these simulations, pairs of phase coupled signals were generated, per Eq. (2). Each of the bivariate signals contains 4096 data points with zero mean, and unit variance. The calculation of the cross-bispectra and cross-bicoherence is based on FFT resolution of 0.0078125 with the segment length of 128 and 50% overlap.

In the first simulation, fully phase coupled signals were generated and a varying level of GWN was added to the signal. In the second simulation, phase coupling was varied from 0 to 100%. For the third simulation, the number of data points was varied in increments of 128. For each simulation, 100 realizations are generated for each condition and an average value was obtained. Further, the specificity of the algorithm was assessed by searching for the total number of significant peaks across each calculation. Theoretically, if the specificity is high, only one peak is shown.

Experimental Procedure

All experiments were performed under protocols approved by The Institutional Animal care and Use Committee at Stony Brook and The University of South Florida. Data were collected from a previous study where stop flow pressure recordings from two nephrons were simultaneously measured in normotensive Sprague-Dawley rats (SDRs, 240–300 g, $n = 15$) and SHRs (weight matched, 12 week old, $n = 18$). Surgical preparation and the stop flow pressure measurements are detailed in our previously published study,[3] thus, will only be briefly described here. Animals were anesthetized with halothane administered in an oxygen–nitrogen mixture and artificially ventilated after the administration of a muscle relaxant. Tubular flow was interrupted with bone wax in a selected proximal tubule, and intratubular hydraulic pressure proximal to the wax block was measured via a 1- to 3-μm diameter micropipette attached to a servo-nulling pressure circuit. A similar procedure was performed onto a second nephron that is in close proximity to the original. Data from the two nephrons were recorded on a TEAC R-61 4-channel cassette data recorder for off-line analysis. The recorded data were replayed through an electronic low-pass filter with a roll-off frequency of 1.5 Hz and sampled digitally at 4 Hz. Vascular connections between nephrons were confirmed with vascular cast after measurement. Nephron pairs that did not show vascular connections were also analyzed to serve as negative control. In total, 9 of the 15 SDRs and 7 of the 18 SHRs show vascular connections under vascular cast.

Data Analysis

Data recorded at a sampling rate of 4 Hz were further down-sampled to 1 Hz after an anti-aliasing low-pass filter at 0.5 Hz. The data were then zero meaned, detrended, and normalized to unit variance in order to facilitate comparison. Since the direction of coupling is unknown between the nephrons, the CBicS method was applied in both directions (e.g., B_{xyx} and B_{yxy}) to search for significant phase coupling. The total number and average magnitude of coupling for each dataset were recorded. As described earlier, all datasets were analyzed regardless of whether physiological

connections were present under vascular cast. Statistical testing was done using student's *t*-test or Mann–Whitney rank sum test.

RESULTS

Test for Normality

Both of the surrogate methods introduced in this study make use of the descriptive statistics of mean and standard deviation, which assumes normality. Therefore, it is important to first confirm that the calculated set of 100 surrogate cross-bispectrum and cross-bicoherence values follows a normal distribution. One hundred realizations of the test signal were generated according to Eq. (2), and 100 surrogate data realizations were generated from each of the 100 test signals. The cross-bispectrum and cross-bicoherence were calculated for each surrogate dataset, and the value at the coupling frequency was recorded. Each of the 100 sets of surrogate data cross-bispectrum and cross-bicoherence were tested for normality using the Kolmogorov–Smirnov goodness of fit test.[21] All of the surrogate datasets were statistically confirmed to be from a normally distributed population ($p > 0.05$).

Case 1: Noise Contamination Simulation

The three method's ability to correctly detect coupling in the presence of noise was tested. In this simulation, varying levels of GWN were used to corrupt the test signal pairs. The noise was varied from 30 to −30 dB, in steps of −1 dB. At each noise level, 100 realizations of the test signal pairs according to Eq. (2) were generated, and each pair was corrupted by an independent pair of GWN. The calculated mean value across the 100 test datasets at the true frequency pairs, and the median number of detected peaks were recorded. The result from this noise simulation is shown in Fig. 2. The top panels show the mean calculated value for each respective method, while the bottom panels show the median number of detected peaks. The dotted line on the top panels shows the threshold for significance for each method. The columns are arranged with cross-bicoherence results on the left, CBS in the middle, and the CBicS on the right.

The cross-bicoherence is able to discern significant phase coupling up to −18 dB of noise. Both surrogate data methods were able to discern significant phase coupling up to the simulation limit of −30 dB of noise. However, the middle bottom panel shows the CBS loses specificity with increasing noise, detecting a median of four peaks at −30 dB. The cross-bicoherence and the CBicS were very specific as both methods never detect more than 1 peak. Therefore, both cross-bicoherence based methods offer great specificity as neither detects erroneous peaks. However, the sensitivity of the cross-bicoherence was less compared to that of the CBS and the CBicS, as it was only able to discern phase coupling up to −18 dB of noise. Taken together, this shows that the CBicS offers the best combination of sensitivity as well as specificity in noise corrupted data.

It is interesting to note that the CBS's behavior with increasing noise is opposite of that of the two cross-bicoherence based methods in that its magnitude of the calculated value increases with increasing noise. A possible explanation for this phenomenon is that since

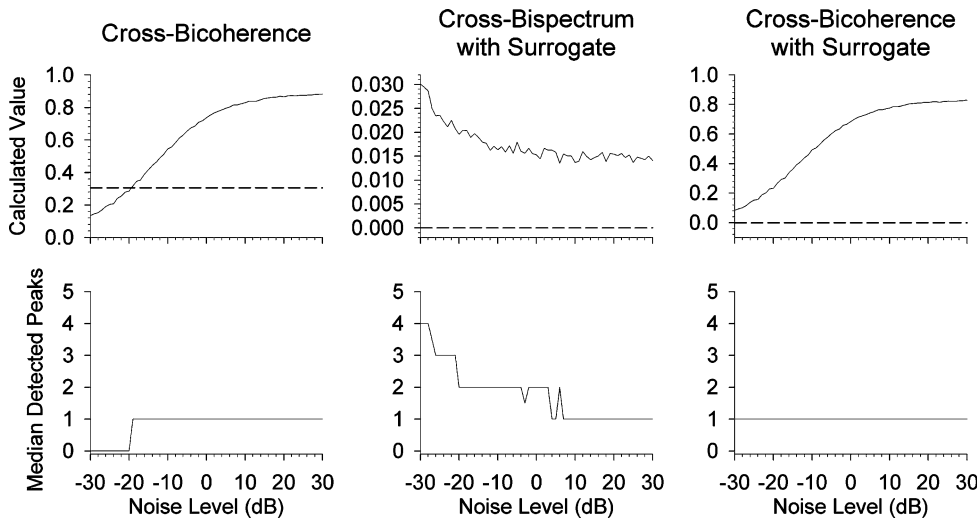

FIGURE 2. Simulation summary to test the three algorithm's efficacy against varying noise levels. The top panels show the calculated value of the respective methods, while the bottom shows the median number of detected peaks. Simulations were performed in steps of 1 dB with 100 realizations at each noise level.

the noise is Gaussian, as the noise level goes up, the magnitude of the cross-bispectra will increase at all frequency pairs, including the magnitude at the frequency of coupling. In contrast, the normalization procedure in the calculation of the cross-bicoherence suppresses this power from non-coupling mechanisms, therefore leading to a decrease in calculated value as the noise increases.

It is important to note that the noise levels (noise variance is ~100 times greater than the variance of the noiseless signal) used in this simulation are generally much higher than that which is normally experienced in real experiments. However, one must keep in mind that the test signals used in this simulation are all designed to specifically be detected by cross-bispectra techniques. Real signals from experiments are never in this form, and hence the algorithm's efficacy may decrease. Therefore, it is important to keep in mind that the results shown here are purely for comparative purposes and not to be used as guidelines for noise tolerance for the algorithms in experimental settings.

Case 2: Coupling Percent Simulation

In this simulation, the amount of phase coupling needed to discern significant phase coupling was compared between the three methods. Test signal pairs were generated according to Eq. (2), with one part of the signal being phase coupled while the other part having random phases. The amount of the signal that was phase coupled was varied between 1 and 100%, in steps of 1%. At each percent, 100 realizations of the test signal pairs were generated. Similar to the previous simulation, the mean calculated value and the median number of detected peaks between the 100 realizations for each percent level were recorded. The results are shown in Fig. 3 and they are arranged the same way as in Fig. 2.

It is important to note that the CBS algorithm was able to detect significant coupling independent of the amount of phase coupling. This highlights a disadvantage of the CBS algorithm in that frequency coupling alone is sufficient for the CBS algorithm to detect as the presence of QPC. The results for the two cross-bicoherence-based methods show that the cross-bicoherence requires that the signals be at least 60% phase coupled. The CBicS, on the other hand, requires only 25% of the data to be coupled for detection. This gives the CBicS a big advantage in that the algorithm can detect weakly phase coupled signals. Further, physiological systems are often time-varying in nature, which may result in signals that have intermittent coupling. This can be seen as a weakly coupled signal, as the phase coupling only exists in selected portions of the data. Again, the CBicS algorithm is able to detect this time-varying coupling better than either the cross-bicoherence or CBS algorithms.

Taking the noise and percent coupling simulation together points to a weakness in the cross-bicoherence based algorithms. It could be seen that the calculated value goes down regardless of whether it is due to increase in noise levels or decrease in coupling percent. Therefore, when the magnitude of the CBicS between two signals is compared, one can never be sure of whether it is due to differences in noise levels or the degree of coupling. This is similar to coherence analysis, where noise and the degree of coherence will both affect the magnitude of the result. Although this may

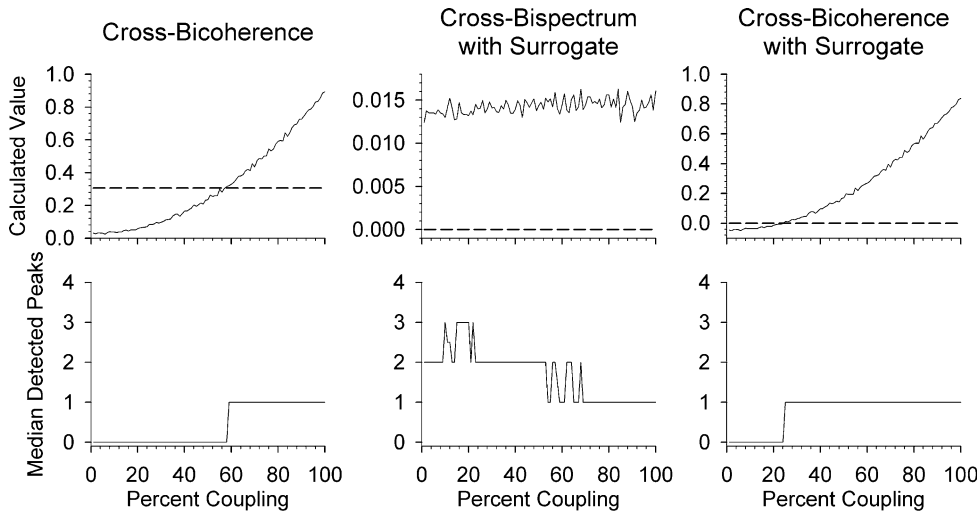

FIGURE 3. Simulation summary to test the three algorithm's efficacy against different percent of coupling. The top panels show the calculated value of the respective methods, while the bottom shows the median number of detected peaks. Simulations were performed in steps of 1%, with 100 realizations at each percent level.

be an inherit weakness in the algorithm, in most experimental cases one can usually assume that the noise levels are comparable between experiments and hence, this should not be an issue. One possible way to resolve this weakness would be to use a time-varying bispectral analysis, as a low coupling percent could be viewed as a time-varying process. In theory, the surrogate approaches could be implemented into a time-varying cross-bispectrum algorithm, allowing for statistical quantification.

Case 3: Data Length Simulation

In this simulation, the data length was varied in order to assess the data length requirements for each algorithm. Phase coupled test signals were generated according to Eq. (2). The data length was varied in steps of 128 points from 128 to 4098 in order to keep the segment number constant at 128. At each data point step, 100 realizations of the test signal pairs were generated and analyzed with the three algorithms. The results are shown in Fig. 4 and arranged in the same way as previous figures. Note that the threshold for the cross-bicoherence in this simulation changes as the number of segments changes.

The results show that the performance of both the cross-bicoherence and CBicS are similar, where the methods are able to discern significant coupling for four and three segments, respectively. The CBS algorithm was able to detect significant coupling with as few as 128 points (1 segment), but detected erroneous peaks with fewer than 2176 points (17 segments). Further, the calculated value for the CBS increased with decreasing data length. These points to a weakness in the CBS algorithm: at low segment numbers, the method loses specificity.

The simulation result for the cross-bicoherence points to a weakness in the segment number-based threshold in that at low segment numbers, the threshold becomes extremely high. This leads to a severe drop in sensitivity at low data points. One possible solution to this problem would be to decrease the segment size to increase the number of segments. However, this will lead to a decrease in resolution, as the segment size determines the frequency resolution. Therefore, one must keep this tradeoff of resolution vs. ability to detect significant coupling in mind while choosing segment size.

The simulation for the CBicS here also points to a potential weakness in the algorithm in that the calculated value decreases drastically with data points less than approximately 1000 points, even though it was able to still correctly detect a single coupling peak with low data points. Therefore, when analyzing physiological data one must keep the data length between datasets similarly sized for comparison.

Experimental Data Results

To reiterate the importance of a statistical method for the analysis of bispectral results, analysis for a representative dataset of anatomically connected nephrons is shown in Fig. 5. The top two panels of Fig. 5 show the stop flow pressure time traces from two simultaneously measured nephrons. The bottom left panel shows the cross-bispectrum of the datasets. Note the large peak shown at the MYO–TGF frequency range (0.13 and 0.023 Hz, respectively).

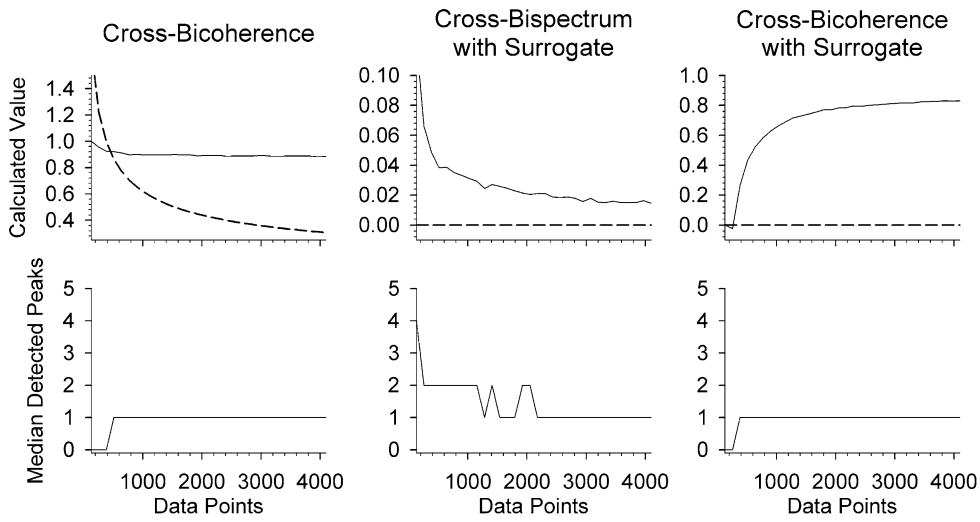

FIGURE 4. Simulation summary to test the three algorithm's efficacy against different number of data points. The top panels show the calculated value of the respective methods, while the bottom shows the median number of detected peaks. Simulations were performed in steps of 128 points, with 100 realizations at each data length.

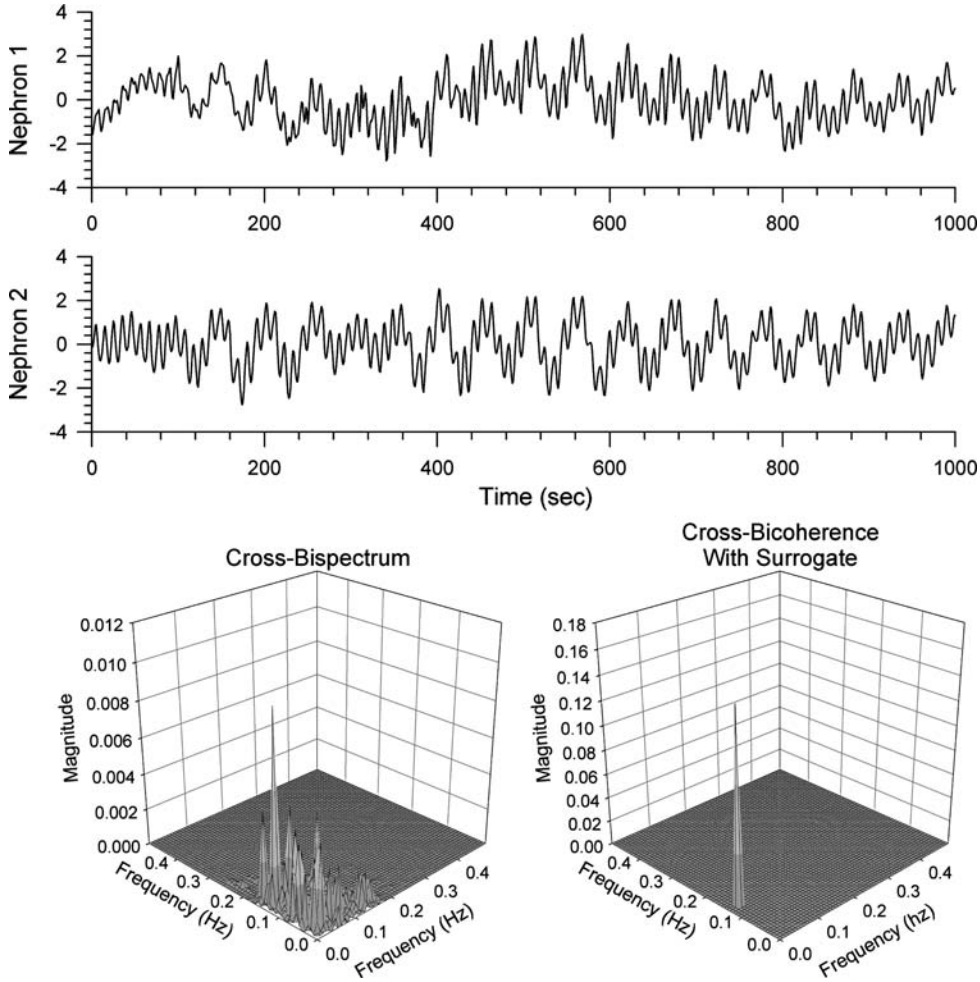

FIGURE 5. Representative data from the stop flow pressure measurements. The top two panels show pressure measurements from two simultaneously measured nephrons. The bottom left panel shows the cross-bispectrum of this pair of data. Note that in addition to a large peak, many other smaller peaks appear, confounding the interpretation of the cross-bispectrum. The bottom right panel shows the result from the application of the cross-bichoerence with a surrogate method. The non-significant peaks shown in the cross-bispectrum are all removed, leaving only one significant true peak.

Further, many other smaller peaks are also present, whose magnitude suggests that they may also be significant peaks, hence complicating the interpretation of data. The bottom right panel shows the result after the application of the CBicS algorithm, which shows a single large peak at the frequencies associated with MYO (0.13 Hz) and TGF (0.023) mechanisms. All of the smaller peaks shown on the cross-bispectrum were eliminated statistically using the CBicS algorithm, therefore allowing for the proper interpretation of data.

To further show the high efficacy of the CBicS algorithm, the data were analyzed for all three methods. From vascular cast, 9 of 15 SDR and 7 of 18 SHR datasets were measured to have a physiological connection. The cross-bicoherence method correctly did not detect coupling from non-physiologically connected nephrons, but it was not able to detect coupling from all physiologically connected nephrons (6 of 9 SDRs and 4 of 7 SHRs). The CBS was able to detect significant coupling from all nephron pairs with physiological connections, but it also detected some coupling from non-physiologically connected nephrons (2 of 6 SDRs and 5 of 11 SHRs). Only the CBicS algorithm correctly detected coupling from all physiologically connected nephrons and no coupling from non-physiologically connected nephrons. These results show a similar outcome to the simulation results, where the cross-bicoherence suffers from low sensitivity, while the CBS suffers from low specificity. This further demonstrates the high sensitivity and specificity of the CBicS algorithm for the determination of significant phase coupling. Therefore, the CBicS was the chosen method for the analysis of the renal flow data.

The summarized results from the analysis of only the nephron pairs that show a physiological vascular

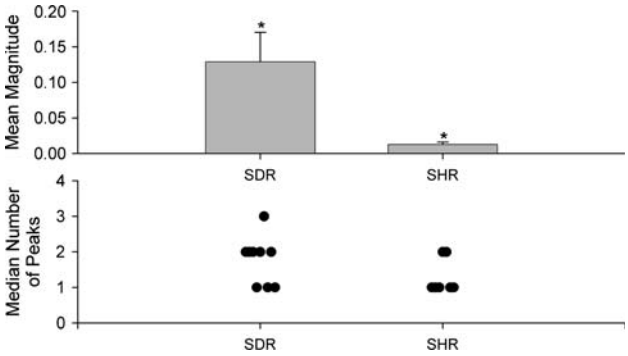

FIGURE 6. Summary results from the stop flow pressure experiment, with $n = 9$ and $n = 7$ for SDR and SHR, respectively. Statistical significance is shown with * ($p \leq 0.05$).

connection are shown in Fig. 6. The top panel of Fig. 6 shows the mean magnitude of coupling across the datasets between the two animal groups, which was shown to be significantly different from each other ($p < 0.05$). The bottom panel of Fig. 6 shows the number of significant peaks from the datasets, which was not significantly different from the normotensive and hypertensive rats.

The CBicS algorithm is able to discern significant phase coupling between nephrons only if they are located on the same cortical radial artery. The nephrons that do not have vascular connections failed to show any significant phase coupling. This would suggest that synchronization between nephrons is achieved via proximity on the vasculature. One possible mechanism for such coupling was originally observed by Schnermann and Briggs[12] and modeled later by Moore *et al.*[8] Basically, the theory is that when one segment of the afferent arteriole undergoes vasoconstriction via renal autoregulatory mechanisms, the pressure in a section of the vasculature upstream of the constriction site will be increased, thereby leading to enhanced response from the autoregulatory mechanisms. If this response is extrapolated to the cortical radial artery, then it may be possible that it is responsible for the coupling observed in this work. Further, this response would naturally decay with increasing distance from the original site of constriction. Therefore, the results here also suggest that the upper limit of distance for this response is at the distance of the cortical radial artery.

Another possible explanation for this coupling phenomenon is that an electrochemical signal is propagated via the vasculature originating from the TGF. Possible methods for this propagation have been proposed as the voltage gated Ca channels[7] or vianitric oxide activity.[4,5]

Although not shown, the coupling detected in this work only existed between TGF and MYO or the self-coupling between MYO and MYO itself. Absent was the coupling between TGF and TGF. This may be a result of experimental condition of the stop flow pressure. In essence, since both nephrons' flow was interrupted via a bone wax plug, each of the nephron's own TGF mechanism was unable to sense the other's activity. On the other hand, since the MYO mechanism sense flow at the level of the afferent arteriole, it is still able to sense and interact with the TGF mechanism. Therefore, this explains the presence of TGF–MYO and MYO–MYO interactions and not TGF–TGF. It is important to note that although only two modes of coupling can occur, more than two peaks can be detected. This is because both TGF and MYO mechanisms can operate in any of the frequency within 0.02–0.5 Hz and 0.1–0.3 Hz bands, respectively. In other words, in certain occasions, they may operate at different frequencies but within the above-defined bands. Thus, in these cases, we can obtain more than two possible couplings.

Given the fact that a rat's kidney is composed of approximately 30,000 nephrons, it is reasonable to expect that nonlinear interactions observed at the whole kidney[2,11] arise from coupling between nephrons derived from the same cortical radial artery.[1,6,20] In a study by Sosnovtseva *et al.*,[17] it was noted that the coupling between nephrons in SHR was shown to be less common in free flow nephrons. While our study differs from them because we used the stop flow pressure data, we still observe decrease in magnitude of coupling in SHR when compared to SDR. A decrease in the degree of coupling can result from intermittent coupling. Indeed, we previously found more intermittent coupling in SHR at the single nephron level.[11] Such intermittent coupling may indicate a time-varying system. Thus, implementing a time-varying version of the algorithm presented here in the future may yet reveal more information about the nature of the coupling phenomenon.

CONCLUSION

In summary, we presented a surrogate data-based approach to statistically quantify QPC based on the cross-bispectrum, adapted from a method we previously developed for the auto-bispectrum. Simulations were used to assess the efficacy of the algorithm along with the traditional method of cross-bicoherence. Simulation results showed that surrogate data technique combined with cross-bicoherence offered the best combination of specificity and sensitivity between the methods compared. These results are in contrast to the results we obtained in an earlier work on the auto-bispectrum, where surrogate data combined with the bispectrum was found to be superior. Application of

this method to renal data revealed nephron-to-nephron interactions when they were derived from the same cortical renal artery. Having at hand the information on the connectivity between the nephrons, we were able to validate the accuracy of CBicS results; it was found that the accuracy was 100%. The CBicS method is a general purpose algorithm, thus it can be adapted to many different physiological signals. For example, quantitative determination of possible loss of coupling during epileptic seizures is an attractive application of the method.

REFERENCES

[1]Chen, Y. M., K. P. Yip, D. J. Marsh, and N. H. Holstein-Rathlou. Magnitude of TGF-initiated nephron-nephron interactions is increased in SHR. *Am. J. Physiol.* 269(2 Pt 2): F198–F204, 1995.

[2]Chon, K. H., Y. M. Chen, V. Z. Marmarelis, D. J. Marsh, and N. H. Holstein-Rathlou. Detection of interactions between myogenic and TGF mechanisms using nonlinear analysis. *Am. J. Physiol.* 267(1 Pt 2):F160–F173, 1994.

[3]Chon, K. H., R. Raghavan, Y. M. Chen, D. J. Marsh, and K. P. Yip. Interactions of TGF-dependent and myogenic oscillations in tubular pressure. *Am. J. Physiol. Renal. Physiol.* 288(2):F298–F307, 2005. doi:10.1152/ajprenal.00164.2004.

[4]Just, A., and W. J. Arendshorst. Nitric oxide blunts myogenic autoregulation in rat renal but not skeletal muscle circulation via tubuloglomerular feedback. *J. Physiol.* 569(Pt 3):959–974, 2005. doi:10.1113/jphysiol.2005.094888.

[5]Just, A., H. Ehmke, U. Wittmann, and H. R. Kirchheim. Tonic and phasic influences of nitric oxide on renal blood flow autoregulation in conscious dogs. *Am. J. Physiol.* 276(3 Pt 2):F442–F449, 1999.

[6]Kallskog, O., and D. J. Marsh. TGF-initiated vascular interactions between adjacent nephrons in the rat kidney. *Am. J. Physiol.* 259(1 Pt 2):F60–F64, 1990.

[7]Marsh, D. J., O. V. Sosnovtseva, K. H. Chon, and N. H. Holstein-Rathlou. Nonlinear interactions in renal blood flow regulation. *Am. J. Physiol. Regul. Integr. Comp. Physiol.* 288(5):R1143–R1159, 2005. doi:10.1152/ajpregu.00539.2004.

[8]Moore, L. C., A. Rich, and D. Casellas. Ascending myogenic autoregulation: interactions between tubuloglomerular feedback and myogenic mechanisms. *Bull. Math. Biol.* 56(3):391–410, 1994.

[9]Nikias, C. L., and A. P. Petropulu. Higher-Order Spectral Analysis: A Nonlinear Signal Processing Framework. Englewood Cliffs, NJ: PTR Prentice Hall, 1993.

[10]Ning, T., and J. D. Bronzino. Nonlinear analysis of the hippocampal subfields of CA1 and the dentate gyrus. *IEEE Trans. Biomed. Eng.* 40(9):870–876, 1993. doi:10.1109/10.245607.

[11]Raghavan, R., X. Chen, K. P. Yip, D. J. Marsh, and K. H. Chon. Interactions between TGF-dependent and myogenic oscillations in tubular pressure and whole kidney blood flow in both SDR and SHR. *Am. J. Physiol. Renal. Physiol.* 290(3):F720–F732, 2006. doi:10.1152/ajprenal.00205.2005.

[12]Schnermann, J., and J. P. Briggs. Interaction between loop of Henle flow and arterial pressure as determinants of glomerular pressure. *Am. J. Physiol.* 256(3 Pt 2):F421–F429, 1989.

[13]Schreiber, T., and A. Schmitz. Improved surrogate data for nonlinearity tests. *Phys. Rev. Lett.* 77(4):635–638, 1996. doi:10.1103/PhysRevLett.77.635.

[14]Shils, J. L., M. Litt, B. E. Skolnick, and M. M. Stecker. Bispectral analysis of visual interactions in humans. *Electroencephalogr. Clin. Neurophysiol.* 98(2):113–125, 1996. doi:10.1016/0013-4694(95)00230-8.

[15]Siu, K. L., J. M. Ahn, K. Ju, M. Lee, K. Shin, and K. H. Chon. Statistical approach to quantify the presence of phase coupling using the bispectrum. *IEEE Trans. Biomed. Eng.* 55(5):1512–1520, 2008. doi:10.1109/TBME.2007.913418.

[16]Sosnovtseva, O. V., A. N. Pavlov, E. Mosekilde, N. H. Holstein-Rathlou, and D. J. Marsh. Double-wavelet approach to study frequency and amplitude modulation in renal autoregulation. *Phys. Rev. E Stat. Nonlin. Soft Matter. Phys.* 70(3 Pt 1):031915, 2004. doi:10.1103/PhysRevE.70.031915.

[17]Sosnovtseva, O. V., A. N. Pavlov, E. Mosekilde, K. P. Yip, N. H. Holstein-Rathlou, and D. J. Marsh. Synchronization among mechanisms of renal autoregulation is reduced in hypertensive rats. *Am. J. Physiol. Renal. Physiol.* 293(5): F1545–F1555, 2007. doi:10.1152/ajprenal.00054.2007.

[18]Theiler, J., S. Eubank, A. Longtin, B. Galdrikian, and J. D. Farmer, Testing for nonlinearity in time series: the method of surrogate data. In: Interpretation of Time Series from Nonlinear Mechanical Systems. Warwick, UK: Elsevier and New York, NY: North-Holland, Inc., 1992, pp. 77–94.

[19]Widman, G., T. Schreiber, B. Rehberg, A. Hoeft, and C. E. Elger. Quantification of depth of anesthesia by nonlinear time series analysis of brain electrical activity. *Phys. Rev. E Stat. Phys. Plasmas Fluids Relat. Interdiscip. Topics* 62(4 Pt A):4898–4903, 2000. doi:10.1103/PhysRevE.62.4898.

[20]Yip, K. P., N. H. Holstein-Rathlou, and D. J. Marsh. Dynamics of TGF-initiated nephron-nephron interactions in normotensive rats and SHR. *Am. J. Physiol.* 262(6 Pt 2): F980–F988, 1992.

[21]Zar, J. H. Biostatistical Analysis. Upper Saddle River, N.J.: Prentice Hall, 1999.